Journal of Materials Chemistry A

PAPER

View Article Online
View Journal | View Issue

Cite this: J. Mater. Chem. A, 2019, 7, 26631

A self-protective, reproducible textile sensor with high performance towards human–machine interactions†

Ling Zhang,[ab] Jiang He,[*bc] Yusheng Liao,[d] Xuetao Zeng,[d] Nianxiang Qiu,[e] Yun Liang,[ab] Peng Xiao[*a] and Tao Chen[*ab]

Received 28th September 2019
Accepted 31st October 2019

DOI: 10.1039/c9ta10744d

rsc.li/materials-a

Textile-based electronic devices have aroused considerable interests due to their excellent flexible, wearable and breathable features towards the next-generation intelligent wearable human–machine interfaces. However, as they are vulnerable to the mechanochemical attacks from sweat, oil, *etc.* or wear and tear, the realization of functional electronic textiles (e-textiles) with simultaneous high performance, environment stability, and mechanical robustness still remains a big challenge. Herein, we designed a self-protective and reproducible e-textile (SPRET) composed of an entangled carbon nanotube (CNT) network, a combined polypyrrole-polydopamine-perfluorodecyltrlethoxysilane (PPy-PDA-PFDS) polymer layer and a textile substrate *via* a hierarchical construction strategy. The achieved SPRET sensor can protect itself from the interference of a variety of agents with superlyophobicity and reproduce after severe machine-washing or tape-peeling cycles with mechanical robustness. In our system, the resulted wearable e-textile could be effectively utilized to monitor human motions, realize intuitive human–machine interactions and robot-learning with sweat/water exposure, showing significant potentials in practical wearable e-textiles for continuous, long-term and reliable human behavior monitoring.

Introduction

Wearable electronics have bloomed over the past few years due to their portable, flexible and lightweight properties, and they are emerging as the next-generation intelligent devices to realize real-time human motion/health monitoring, human–machine/brain communications and robot-learning.[1–5] As indispensable components, electronic textiles (e-textiles) are equipped with compelling features of being breathable, flexible/stretchable, comfortable, sewable, deformable, and washable, providing great prospects for comfortable and smart wearable electronic devices.[6–10] In recent years, extensive efforts have been dedicated to textile-based wearable sensing systems.[11–14] For example, in terms of the favorable complex deformability of textiles, Wang *et al.* have developed an all-textile pressure sensor with high sensitivity.[15] Zhang *et al.* have fabricated an elastomer-encapsulated carbonized silk textile that functions as a strain sensor with ultra-stretchable and highly sensitive performance.[16] However, e-textiles on human body are vulnerable to mechanochemical attacks from the external environment, which may experience sweat, oil, water, drinks or wear and tear as well as severe washing cycles. Thus, a textile-based wearable sensing system must possess three important features: high performance, environment stability in both air and water/wet conditions, and mechanical robustness under harsh abrasion or washing.

A superwettability system has been constructed for practical and potential applications in self-cleaning,[17] chemical shielding,[18] anti-fouling,[19] anti-corrosion,[20] anti-fogging,[21] *etc.* Incorporated with superwettability, wearable sensors can survive from sweat corrosion or other agents' attacks for reliable and continuous monitoring.[22,23] Moreover, the hierarchical structures of superwettable surfaces are fragile and the adhesion between the functional coating and the substrate is weak. Such an artificial surface may quickly withdraw its effective protection during daily use of continuous wear and tear.[24,25] In addition, the conductive coverage requires mechanical robustness as well.[26,27] Electroactive nanomaterials, such as carbon nanotubes,[15] graphene,[28] carbon black[29] and Ag nanowires,[30] have been explored for constructing textile sensors *via* coating

[a]Key Laboratory of Marine Materials and Related Technologies, Zhejiang Key Laboratory of Marine Materials and Protective Technologies, Ningbo Institute of Material Technology and Engineering, Chinese Academy of Sciences, Ningbo, 315201, China. E-mail: xiaopeng@nimte.ac.cn; tao.chen@nimte.ac.cn

[b]School of Chemical Sciences, University of Chinese Academy of Sciences, 19A Yuquan Road, Beijing 100049, China

[c]Beijing Institute of Nanoenergy and Nanosystems, Chinese Academy of Sciences, Beijing 100083, China. E-mail: hejiang@binn.cas.cn

[d]Zhejiang Key Laboratory of Robotics and Intelligent Manufacturing Equipment Technology, Ningbo Institute of Materials Technology and Engineering, Chinese Academy of Sciences, Ningbo 315201, China

[e]Engineering Laboratory of Nuclear Energy Materials, Ningbo Institute of Materials Technology and Engineering, Chinese Academy of Sciences, Ningbo 315201, China

† Electronic supplementary information (ESI) available. See DOI: 10.1039/c9ta10744d

strategies. However, these materials can hardly meet the requirements of daily abrasion due to the weak interactions between them and the fibers. Moreover, it is important to note that the conductive and the superwettable layers are interlocked. Superwettable components usually degrade the conductivity of electroactive materials.[31] Consequently, the construction of a textile sensor with the simultaneous demonstration of high sensing performance, mechanical robustness and superwettability remains a big challenge.

In this study, we developed a self-protective and reproducible e-textile (SPRET) *via* hierarchically constructing a "steels-concrete" structured nanocomposite as a robust superlyophobic sensing layer on textile. The as-prepared SPRET consists of "steels" of conductive CNT network and "concrete" of multifunctional polymers (polypyrrole-polydopamine-perfluorodecyltrlethoxysilane, PPy-PDA-PFDS), exhibiting desirable superlyophobicity to a variety of agents, mechanical durability under machine-washing, tape-peeling, and high-sensitive performance (Fig. 1a). When integrated into an all-textile pressure sensor (Fig. 1b), a series of human motions and physiological signals could be precisely and soundly detected either in air/wet conditions or underwater. Furthermore, it was utilized to realize human–machine interactions and robot-learning systems (Fig. 1c) with sweat and/or water exposure.

Results and discussion

Material fabrication

Fig. 2a illustrates the fabrication procedures and the refined structure of SPRET. The main procedure includes three steps: (i) oxygen plasma treatment of polyethylene terephthalate (PET) textiles, (ii) coating of conductive CNT "steels" network on the fiber surfaces, and (iii) *in situ* reaction of a multifunctional polymer "concrete" on the CNT coated e-textile (CCET). After the oxygen plasma surface treatment in the first step, hydroxyl groups (–OH) are formed on the PET fiber surfaces. Due to these hydrophilic groups, the CNT ink could thoroughly wet the textile to form uniform "steels" like conductive networks on each fiber (Fig. 2b and S1†). Through the *in situ* reaction, "concrete" like polymer composite is introduced to fix the "steels" (Fig. 2e and S1†) to anchor them to the fibers (Fig. 2a-iv) and to lower the surface energy of the textile, which is critical to the mechanical robustness, and the superlyophobic and sensitive behaviors of the e-textiles. In our formulation, mussel-inspired PDA was chosen to react with the fiber surfaces and strongly wrap the CNT "steels" with conductive PPy.[32] The strong interactions among CNTs, PDA and PPy were further investigated by molecular simulations (Fig. S2†). In addition, 1*H*,1*H*,2*H*,2*H*-perfluorodecyltrlethoxysilane (PFDS) with a low surface energy was chemically bonded to the PDA component (Fig. 2a-v and S3†) and uniformly distributed on the fiber surfaces (Fig. 2f). Moreover, a series of subsequent tests were employed to probe the relationship between the structures and the superlyophobic performance of SPRET as well as mechanical durability and sensing behaviors. In addition, with the "steels-concrete" like coverage on each fiber (Fig. 2c), the as-prepared textile exhibits intact flexibility (Fig. 2b) and breathability (Fig. S4†), demonstrating a favourable preservation of the superior features of textile.

Fig. 1 A self-protective, reproducible e-textile with high sensitivity. (a) With multifaceted features, this robust e-textile could survive from sweat, oil, water, drinks, acid and even fierce washing cycles. It could be further integrated into fabric devices (b) for real-time health monitoring, human–machine interactions and robot-learning system with sweat and/or exposure (c).

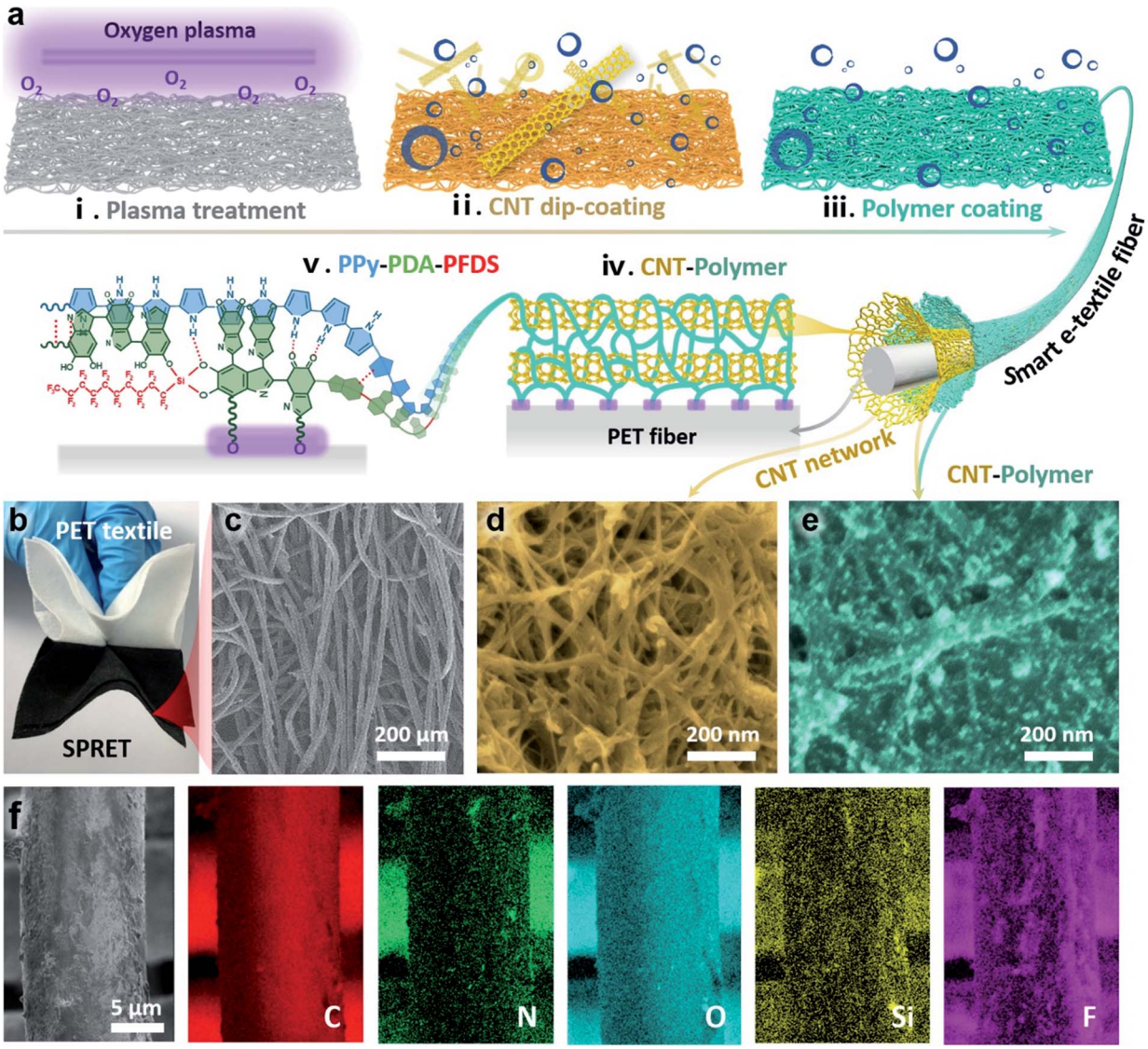

Fig. 2 The fabrication of SPRET. (a) Schematic of the fabrication and the structure of SPRET. (b) Photograph of a virgin PET textile and SPRET. Scanning electron microscope images of SPRET (c) and CNT network (d) or CNT-polymer composite (e) on a fiber. (f) Energy dispersion spectroscopy element mapping images of carbon, nitrogen, oxygen, silicon and fluorine elements in SPRET.

Robust superlyophobicity

Our SPRET is capable of superlyophobicity and mechanical durability. First, we investigated the effect of the chemical formulation of the polymer coverage on the superlyophobicity of SPRET. CCET coated with various chemical modifications, including PFDS, PDA-PPy, and PPy-PDA-PFDS, exhibit superhydrophobic behaviors with the Cassie–Baxter mode in the contact angle (CA) test (Fig. 3a, blue curve). These high CA values (>150°) are attributed to the hierarchical surface textures that are included in the re-entrant structure of textile surfaces and nanostructure on each fiber. However, as for the invasive agents of low surface tension (such as oil), PPy-PDA-PFDS modified sample (SPRET) provides the best performance with an oil CA value of 160.3°, implying an ultralow surface energy of it (Fig. 3a, orange curve). These results suggest that the chemical composition, which is the other crucial factor in addition to the hierarchical structure for constructing a superwettability system, is important in our approach. Compared to the CCET modified by PPy-PDA, the high fluorination degree of PPy-PDA-PFDS makes SPRET super-repellent to both oil and water. However, the fluorinated CCET exhibits an unaltered lipophilicity, which is attributed to the chemical inertness of CNTs and the invalid fluorination. Notably, such a superamphiphobicity of SPRET is a result of its ultralow surface energy, which is determined by the micro/nano structure and the chemical composition. Besides, SPRET shows a lyophobicity (Fig. 3d) and self-cleaning behavior (Fig. 3b and Movie S1†) in response to a broad range of probe liquids of different surface tensions, polarities, and corrosiveness (including saline, tea, vinegar, sweat, coffee, milk, and oil). Furthermore, in the dynamic wetting test of splashing-resistance, a harsh impactive waterspout spreads away without impaling the textile (Fig. 3c),

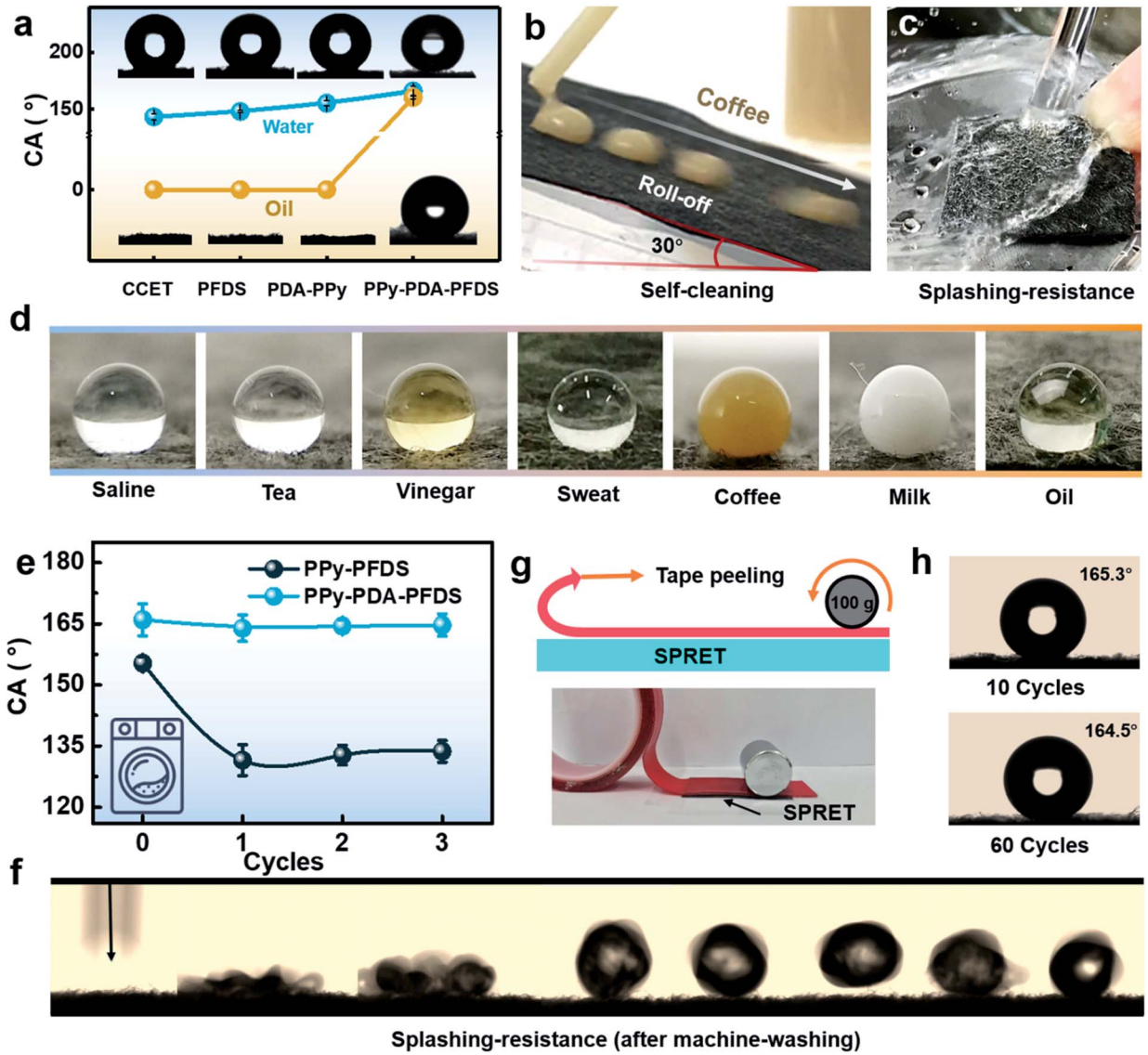

Fig. 3 Superlyophobic performance and washability of SPRET. (a) The contact angles of a series of CCET samples modified by various chemical components. Dynamic wetting tests with coffee rolling from the ~30° inclined SPRET (b) and the impactive waterspout (c). (d) Super-repellency to various liquids. (e) Washing durability test proves that the PDA component provides a robust superlyophobicity to SPRET. (f) Droplet bouncing behavior on SPRET after 3 cycles of washing. CA performance (h) after the mechanical robustness test of tape-peeling cycles (g).

which demonstrates that SPRET is endowed with outstanding superlyophobic performance.

Furthermore, we investigated the effect of PDA on the mechanical durability of SPRET *via* machine-washing and tape-peeling tests. As shown in Fig. 3e and S5,† SPRET presents an almost unaltered water or oil CA value (CA > 150°) after 3 cycles of washing, while the CA of CCET modified by PPy-PFDS decreases sharply after only a 1 cycle of washing. These results suggest a key role of PDA in the washing durability of SPRET. The robust superlyophobic performance of SPRET was further assessed under a harsh condition using sticky polymer paint. The test was performed periodically by blade coating the paint onto the SPRET surface, followed by washing the sample (Fig. S6†), recording the values of CA, sliding angles (SA) and splashing-resistant performance of it. On the surface of SPRET, a CA value of greater than 150°, a SA value of smaller than 10° (Fig. S6†) and the droplet bouncing behavior (Fig. 3f and Movie S2†) are maintained after 3 cycles of washing. Moreover, in a mechanical robustness test of repetitive tape-peeling (Fig. 3g), a high tack tape (VHB, 3 M) was used to assess the coating degradation. After ten peel-off cycles, the sample presents a negligible CA difference while 30 cycles caused a slight drop in CA from 1° to 2° (Fig. 3h). Such an excellent superlyophobic behavior is attributed to the robust "steels-concrete" like coverage.

Sensing performance and mechanical robustness

Favorable conductivity and mechanical durability are desirable for wearable e-textiles, yet they are hard to be achieved

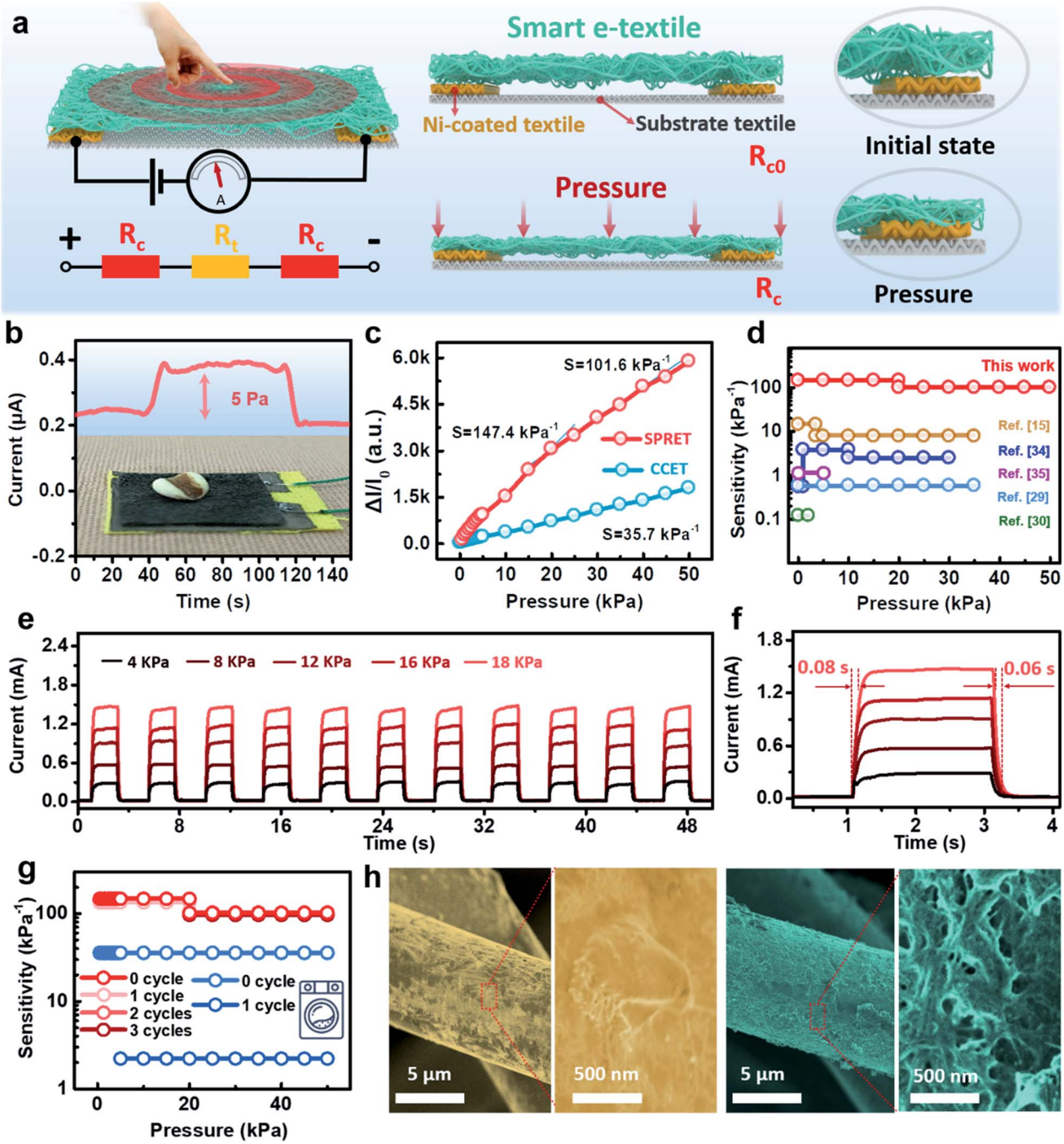

Fig. 4 The fabrication of pressure sensors and the evaluation of its performance. (a) Schematic illustration of the structure and the sensing mechanism of the SPRET sensor. (b) The current response to a coix seed, corresponding to low pressure of ~5 Pa. (c) Pressure-response sensitivity curves for sensors constructed with CCET (blue) and SPRET (red). (d) The sensitivity of the SPRET device in comparison to other previously reported textile-based sensors. Current response curves to various applied pressures during a repetitive loading–unloading process (e) and the details of it demonstrate the respond/recovery time of the SPRET sensor (f). (g) The sensitivity curves of SPRET (red) and CCET (blue) sensors after each washing cycle. (h) Typical SEM images of the morphology of CCET and SPRET after a cycle of washing.

simultaneously. Next, we investigated the possibility of leveraging the PPy-PDA-PFDS "concrete" to enhance the sensing and the mechanical robustness of the e-textiles. As shown in Fig. 4a, SPRET was placed onto a piece of substrate textile with interdigital electrodes of nickel textile. The resistance of the device is a sum of inherent resistance of SPRET (R_t) and the contact resistance (R_c) that refers to the resistance between the top e-textile and the bottom electrodes. With external pressure, fibrous SPRET is of compressive deformation, which results in more fiber-to-fiber contacts and a decreased R_t. In addition, the contact sites between SPRET and the electrodes are increased as well, leading to a dramatic decrease in R_c. With the SPRET

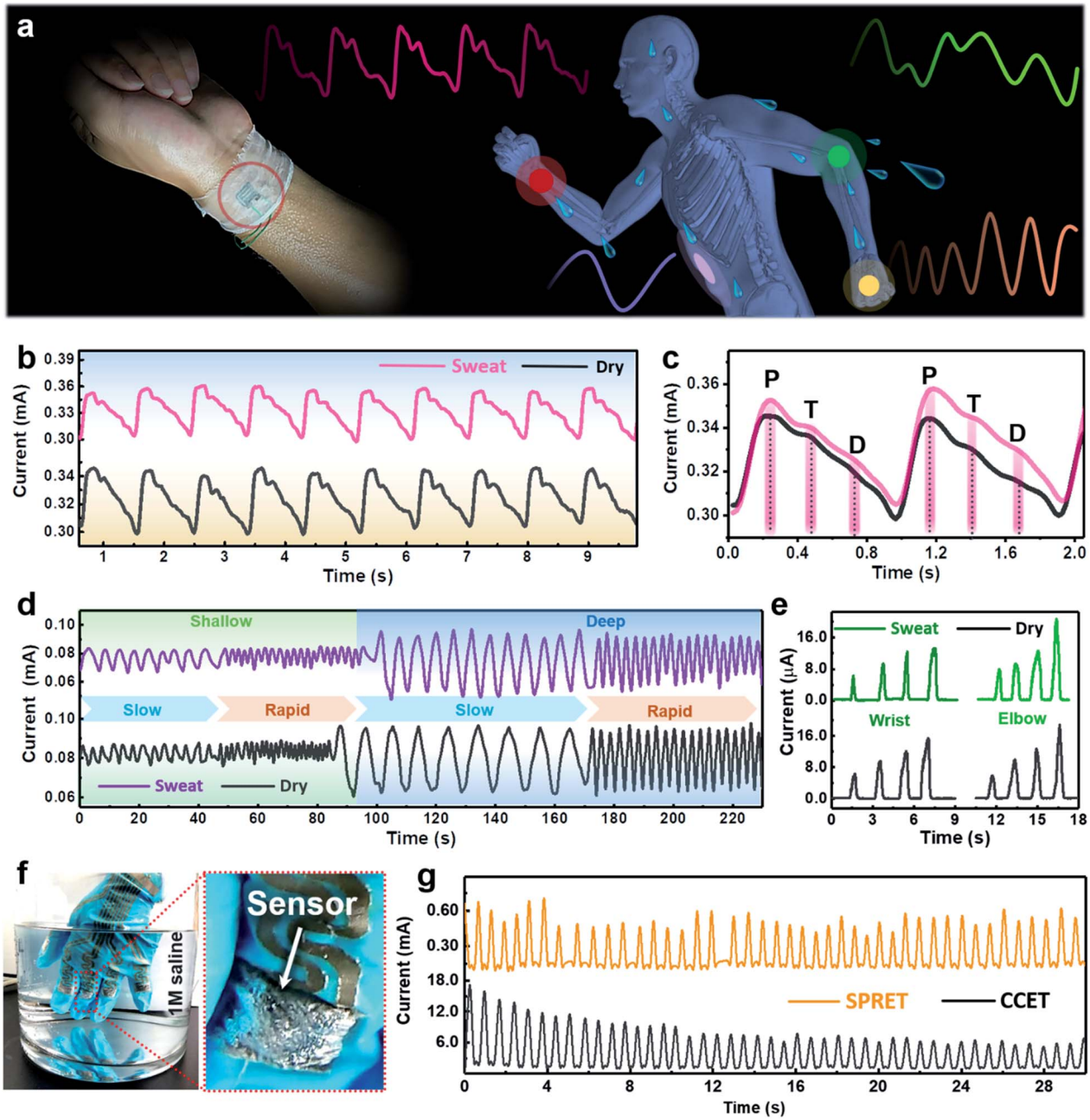

Fig. 5 Detecting human motion on sweaty skin and under extreme aqueous conditions. (a) Schematic of SPRET attached to various positions (including wrist, abdomen, elbow and finger joints) of a sweaty sportsman. Signal of wrist pulse monitoring (b) and its local magnification (c). Detection curves of respiration (d), elbow and wrist bending (e). (f) Typical photographs of SPRET sensors performed under 1 M saline. (g) The current curves of SPRET and CCET sensors in response to finger bending under saline.

sensor being sensitive to external force vibrations, it demonstrates a very low detection limit of ~5 Pa (Fig. 4b).

The sensitivity tests were conducted using a previously reported method.[33] First, a thin glass plate, equal to the size of the device, was placed on it to stabilize the contact area between SPRET and electrodes. The pressure from the glass and e-textile was named as the 'base pressure', corresponding to the initial current (I_0). Second, with additional pressure (p) applied, its corresponding current was recorded as I. Then, the sensitivity was defined as the following equations:

$$S = \delta(\Delta I/I_0)/\delta p,\ \Delta I = I - I_0.$$

As shown in Fig. 4c and S7,† the SPRET sensor shows a quasi-bilinear dependence on the applied pressure: it performs a very high sensitivity (147.4 kPa^{-1}) at the low-pressure region (<20 kPa), and a relatively low value (101.6 kPa^{-1}) in the higher sensing range (20–50 kPa). On the contrary, the sensor of CCET without a polymer coating shows a much lower sensitivity (35.6 kPa^{-1}) in the whole sensing range. According to the definition

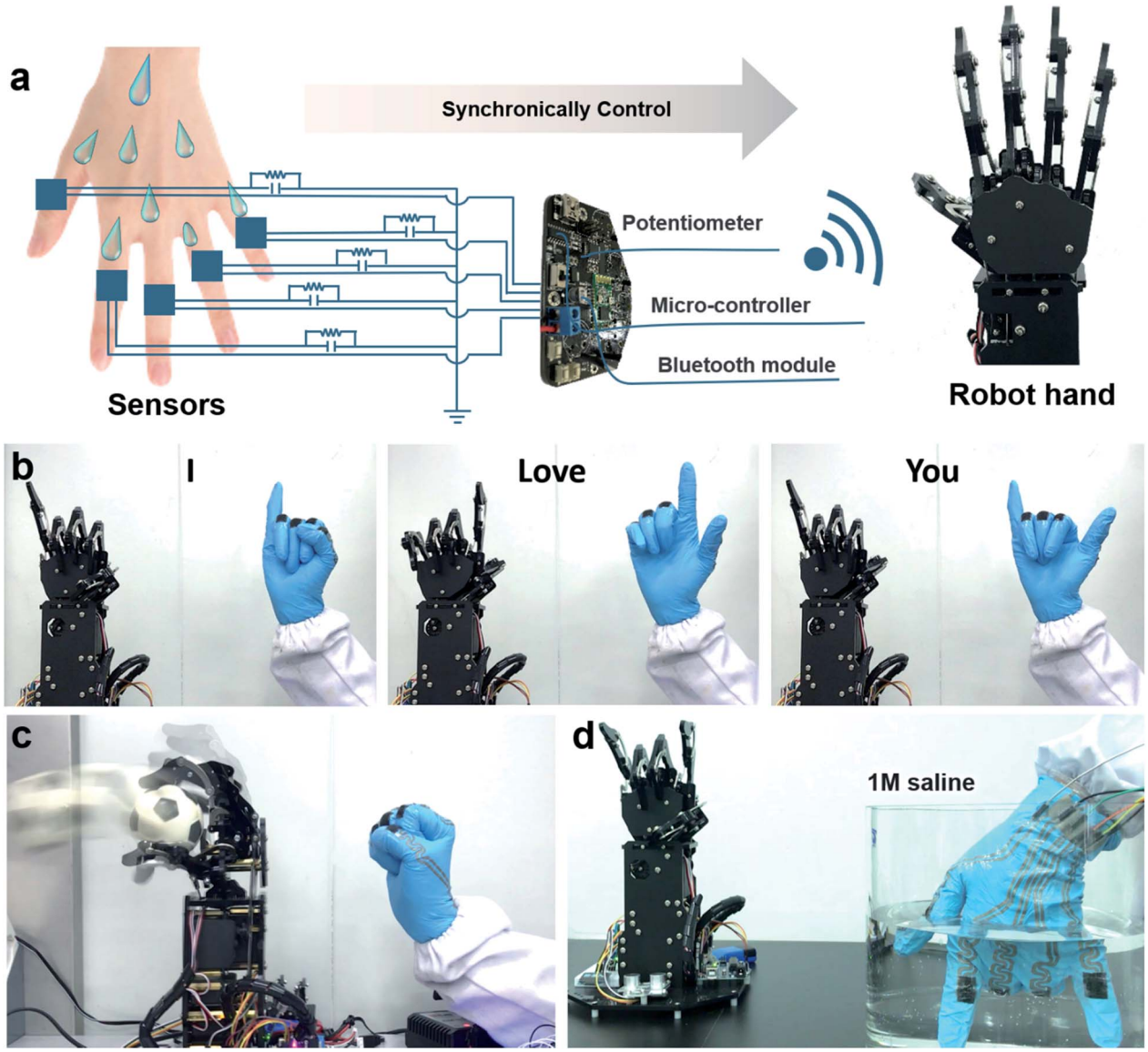

Fig. 6 Intuitive human–robot interaction. (a) Images and schematic illustration of the intuitive human–robot interaction. (b) Demonstration of the machine hands controlled by human hand gestures. (c) The machine hand grasped a flying ball successfully in response to a synchronous human hand. (d) The robot hand responded to the hand under saline.

of sensitivity above, we can attribute such a high sensing performance of SPRET to its favorable conductivity (20 MΩ), which is 2 orders of magnitude lower than that of CCET (160 kΩ). These results prove that our rationally designed polymer nanocoating is beneficial to the sensing performance of the e-textile. In addition, the sensitivity of our device is comparable to or higher than that of other piezoresistive textile/thread-based sensors, including Mxene-,[34] CNT-,[15] Au nanowire-,[35] carbon black[29]-decorated textiles, and Ag nanowire[30] coated threads (Fig. 4d). Furthermore, the repetitive loading–unloading test shows good repeatability, fast response (~80 ms) and recovery time (~60 ms) of the SPRET sensor in response to different pressures (Fig. 4e and f). The stability of it was investigated through a long-time loading–unloading test. After 3000 compressive cycles with pressures between 0 and 100 Pa, no visible degradation in the response current is observed (Fig. S8†), indicating that the electroactive material of CNTs is preserved intact.

To investigate the effect of the polymer coating on the washing durability of e-textiles, CCET and SPRET were tested in the same machine-washing process. As shown in Fig. 4g (blue curve), the sensibility of the CCET sample disappeared due to the peeling-off of the conducting CNT network (Fig. 4h, left). Moreover, the SPRET sustained fierce machine-washing of 3 cycles with the protection of the polymer "concrete" (Fig. 4g, red curve; Fig. 4h, right). Hours of stir-washing was further performed with SPRET, demonstrating the negligible variation of sensitivity (Fig. S9†). Based on these results, we consider that the well-designed PPy-PDA-PFDS coating endows the SPRET device with mechanical durability and a favorable reproducibility.

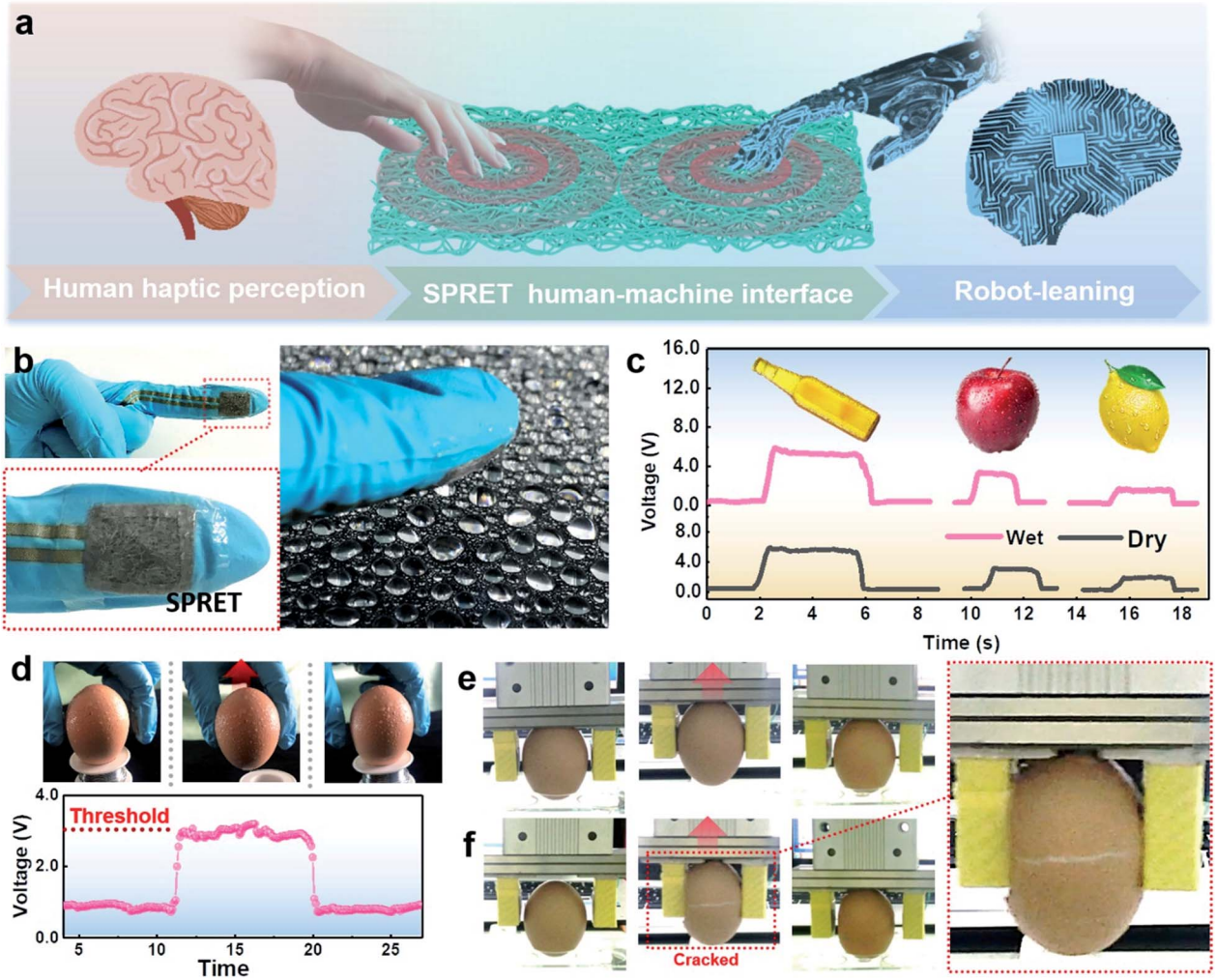

Fig. 7 Application of SPRET in the robot-training system. (a) Schematic illustration of the robot-leaning system. (b) Photographs of a SPRET-armed fingertip and a wetted surface. The smart SPRET finger cot in response to the human grasp of a bottle, an apple and a lemon (c) and an egg (d). In this process, the SPRET finger cot transformed human sensing information into electrical signals, which can be read and learned by the robot. An egg was transferred successfully by the trained robot (e) and crushed by the untrained robot (f).

Monitoring of vital signals with wearable SPRET devices

Wearable devices are increasingly appealing in modern non-invasive individual medical diagnosis as they monitor human motion *via* intimate skin contacts. Thus, the effect of the skin condition should be deliberately taken into consideration. Here, we investigated the practical performance of SPRET devices on the skin using artificial sweat. Our sensors were integrated into a comfortable all-textile system for vital signal monitoring (Fig. 5a). Pieces of riband were selected as the substrate textile for the SPRET sensors, which would assist to attach/detach devices to/from the human skin conveniently. A sensor was placed over the wrist arteries of a calm 27 year-old man for pulse motoring under both dry and sweaty conditions. Percussion wave (P-wave), tidal wave (T-wave) and diastolic wave (D-wave), the key information for cardiovascular disease diagnosis, could be precisely identified under both conditions (Fig. 5b). As shown in Fig. 5c, the enlarged profiles of the pulse waves demonstrate that negligible differences could be identified between dry and sweaty conditions, indicating that sweat has no free effect on the sensing performance of the SPRET. Applications in respiratory monitoring (Fig. 5d) and joint-motion detection (Fig. 5e) further prove its excellent sweat-resistant property in real-life scenarios.

To further demonstrate the insensitivity of SPRET devices to sweat corrosion, an extreme saline immersion test was performed. 1 M saline was selected to mimic conductive sweat. As shown in Fig. 5f, bright air layers are aggregated on the surface of SPRET, which preserve the electronic devices from saline invasion during a consecutive finger bending process (Fig. 5g, orange curve). In contrast, the response current of the CCET sample is dramatically decreased with saline impaling (Fig. 5g, black curve). Furthermore, the SPRET glove performs normally with the consecutive droplet splashing of saline (Fig. S10†). In addition, a quantitative study on finger bending monitoring (Fig. S11†) and sequential gesture recognition (Fig. S12†) were conducted in both air and saline, indicating negligible variation

as well. Consequently, we consider that the SPRET sensor is capable of self-protection, demonstrating its outstanding reliability in practical applications.

Intuitive human–robot interaction

Gesture is considered as an interaction technique that can potentially deliver more natural, creative and intuitive methods for communicating with our computers or robotics. Here, we developed a human–robot interaction system, which was based on a smart glove armed with the SPRET sensor array. As shown in Fig. 6a, a voltage divider circuit was constructed to integrate the SPRET glove with a custom-made data acquisition (DAQ) system and a robot hand. When a SPRET glove-armed hand gestured, the circuit converted the hand motion information to electrical signals for the DAQ system. Recording the raw analog voltage signals by a potentiometer, the DAQ system processed the voltage signals within a microcontroller and communicated with the robot hand through Bluetooth. As shown in Fig. 6b, each finger of the robot was controlled synchronously by the human fingers, which expressed 'I', 'love', 'you' with three sequential gestures. In a human–robot cooperation test, the robot hand precisely captured a flying ball in response to the synchronous human hand (Movie S4† and Fig. 6c). Moreover, benefiting from the self-protective behavior of SPRET sensors, the robot successfully gestured 'I love you', responding to the hand under saline (Fig. 6d).

Application of SPRET in a robot-training system

Capable of haptic perception, human beings are good at manipulating objects rationally, which provides robots with learning paradigm (Fig. 7a). Here, based on a finger cot with an attached SPRET sensor (Fig. 7b), we successfully collected empirical data of human grasp under wet or dry conditions. Notably, with the superlyophobicity of SPRET sensors, a broader database would be acquired. As shown in Fig. 7c, the gripping forces of three elements, including a wine bottle, an apple, and a lemon were transformed into corresponding voltages. The maximum thresholds of voltages, referring to the maximum gripping forces, were recorded for data acquisition. With this database, a robot training system was constructed for element grasp, composed of a two-finger robot with an attached SPRET sensor, a drive-controller (DC), a microcontroller and a host computer (Fig. S13†).

As a proof of concept, the training of egg grasp was conducted in our experiment. From the recorded curve of human manipulation (Fig. 7d), we extracted the voltage value of 3 V as a threshold that was further written into a program in the microcontroller. Then, the two-finger robot was driven by a host computer through DC. As it approached the egg gradually, real-time feedback voltages were sent to the microcontroller for the next processing. When the voltage value achieved 3 V, the microcontroller gave a 'stop' instruction to the DC, preserving the egg from the robot fingers (Fig. 7e). For comparison, another egg was cracked with the system out of training (Fig. 7f).

Conclusions

In conclusion, we have developed self-protective and reproducible e-textiles by a hierarchical construction strategy, in which the superlyophobicity, mechanical durability, and high-sensitive features have been effectively and synergistically integrated into favorable textiles. These e-textiles can protect themselves from the interference of sweat, oil, *etc.*, and reproduce after severe washing and tape-peeling cycles, representing continuous, stable and precise real-time monitoring of human motion and physiological signals under wet/water conditions. Furthermore, owing to the desirable self-protective behaviors of our e-textiles, intuitive human–machine communications, and smart robot-learning systems were readily achieved with sweat/water exposure. In view of the superior sensibility in harsh settings, as well as the soft, breathable and comfortable features, the proposed SPRET sensor holds practical application potential in wearable health monitoring, human–machine interaction, and robot-learning fields.

Conflicts of interest

There are no conflicts to declare.

Acknowledgements

This work was supported by the Natural Science Foundation of China (51803226, 51573203, and 51503216), the Bureau of International Cooperation of Chinese Academy of Sciences (174433KYSB20170061), Key Research Program of Frontier Science, Chinese Academy of Sciences (QYZDB-SSW-SLH036), Postdoctoral Innovation Talent Support Program (BX20180321), China Postdoctoral Science Foundation (2018M630695) and Ningbo Science and Technology Bureau (2018A610108).

Notes and references

1 A. Chortos, J. Liu and Z. Bao, *Nat. Mater.*, 2016, **15**, 937.
2 R. Guo, Y. Yu, J. Zeng, X. Liu, X. Zhou, L. Niu, T. Gao, K. Li, Y. Yang, F. Zhou and Z. Zheng, *Adv. Sci.*, 2015, **2**, 1400021.
3 Z. Zhang, Y. Zhang, X. Jiang, H. Bukhari, Z. Zhang, W. Han and E. Xie, *Carbon*, 2019, **155**, 71.
4 J. Cao, C. Lu, J. Zhuang, M. Liu, X. Zhang, Y. Yu and Q. Tao, *Angew. Chem., Int. Ed.*, 2017, **56**, 8795.
5 Y. Li, D. Han, C. Jiang, E. Xie and W. Han, *Adv. Mater. Technol.*, 2019, **4**, 1800504.
6 K. Dong, X. Peng and Z. L. Wang, *Adv. Mater.*, 2019, e1902549.
7 W. Weng, P. Chen, S. He, X. Sun and H. Peng, *Angew. Chem., Int. Ed. Engl.*, 2016, **55**, 6140.
8 J. Lee, H. Kwon, J. Seo, S. Shin, J. H. Koo, C. Pang, S. Son, J. H. Kim, Y. H. Jang, D. E. Kim and T. Lee, *Adv. Mater.*, 2015, **27**, 2433.
9 C. Zhu, Y. Li and X. Liu, *Polymers*, 2018, **10**, 573.

10 Z. Yin, M. Jian, C. Wang, K. Xia, Z. Liu, Q. Wang, M. Zhang, H. Wang, X. Liang, X. Liang, Y. Long, X. Yu and Y. Zhang, *Nano Lett.*, 2018, **18**, 7085.
11 J. Foroughi, G. M. Spinks, S. Aziz, A. Mirabedini, A. Jeiranikhameneh, G. G. Wallace, M. E. Kozlov and R. H. Baughman, *ACS Nano*, 2016, **10**, 9129.
12 S. Seyedin, J. M. Razal, P. C. Innis, A. Jeiranikhameneh, S. Beirne and G. G. Wallace, *ACS Appl. Mater. Interfaces*, 2015, **7**, 21150.
13 S. Afroj, N. Karim, Z. Wang, S. Tan, P. He, M. Holwill, D. Ghazaryan, A. Fernando and K. S. Novoselov, *ACS Nano*, 2019, **13**, 3847.
14 S. Pyo, J. Lee, W. Kim, E. Jo and J. Kim, *Adv. Funct. Mater.*, 2019, **29**, 1902484.
15 M. Liu, X. Pu, C. Jiang, T. Liu, X. Huang, L. Chen, C. Du, J. Sun, W. Hu and Z. L. Wang, *Adv. Mater.*, 2017, **29**, 1703700.
16 C. Wang, X. Li, E. Gao, M. Jian, K. Xia, Q. Wang, Z. Xu, T. Ren and Y. Zhang, *Adv. Mater.*, 2016, **28**, 6640.
17 Y. Lu, S. Sathasivam, J. Song, C. R. Crick, C. J. Carmalt and I. P. Parkin, *Science*, 2015, **347**, 1132.
18 S. Pan, A. K. Kota, J. M. Mabry and A. Tuteja, *J. Am. Chem. Soc.*, 2013, **135**, 578.
19 A. K. Epstein, T.-S. Wong, R. A. Belisle, E. M. Boggs and J. Aizenberg, *Proc. Natl. Acad. Sci. U. S. A.*, 2012, **109**, 13182.
20 E. Hermelin, J. Petitjean, J.-C. Lacroix, K. I. Chane-Ching, J. Tanguy and P.-C. Lacaze, *Chem. Mater.*, 2008, **20**, 4447.
21 X. Gao, X. Yan, X. Yao, L. Xu, K. Zhang, J. Zhang, B. Yang and L. Jiang, *Adv. Mater.*, 2007, **19**, 2213.
22 L. Li, Y. Bai, L. Li, S. Wang and T. Zhang, *Adv. Mater.*, 2017, **29**, 1702517.
23 P. Wang, B. Sun, Y. Liang, H. Han, X. Fan, W. Wang and Z. Yang, *J. Mater. Chem. A*, 2018, **6**, 10404.
24 T. Wang, Y. F. Si, S. Q. Luo, Z. C. Dong and L. Jiang, *Mater. Horiz.*, 2019, **6**, 294.
25 Y. Li, M. Ren, P. Lv, Y. Liu, H. Shao, C. Wang, C. Tang, Y. Zhou and M. Shuai, *J. Mater. Chem. A*, 2019, **7**, 7242.
26 Z. Zhao, C. Yan, Z. Liu, X. Fu, L. M. Peng, Y. Hu and Z. Zheng, *Adv. Mater.*, 2016, **28**, 10267.
27 R. Cao, X. Pu, X. Du, W. Yang, J. Wang, H. Guo, S. Zhao, Z. Yuan, C. Zhang, C. Li and Z. L. Wang, *ACS Nano*, 2018, **12**, 5190.
28 Z. Yang, Y. Pang, X. L. Han, Y. Yang, J. Ling, M. Jian, Y. Zhang, Y. Yang and T. L. Ren, *ACS Nano*, 2018, **12**, 9134.
29 N. Luo, W. Dai, C. Li, Z. Zhou, L. Lu, C. C. Y. Poon, S.-C. Chen, Y. Zhang and N. Zhao, *Adv. Funct. Mater.*, 2016, **26**, 1178.
30 Y. Wei, S. Chen, X. Yuan, P. P. Wang and L. Liu, *Adv. Funct. Mater.*, 2016, **26**, 5078.
31 G. Ding, W. Jiao, R. Wang, Z. Chu and Y. Huang, *J. Mater. Chem. A*, 2019, **7**, 12333.
32 J. He, P. Xiao, J. Shi, Y. Liang, W. Lu, Y. Chen, W. Wang, P. Théato, S.-W. Kuo and T. Chen, *Chem. Mater.*, 2018, **30**, 4343.
33 J. He, P. Xiao, W. Lu, J. W. Shi, L. Zhang, Y. Liang, C. F. Pan, S. A. W. Kuo and T. Chen, *Nano Energy*, 2019, **59**, 422.
34 Y. Guo, M. Zhong, Z. Fang, P. Wan and G. Yu, *Nano Lett.*, 2019, **19**, 1143.
35 S. Gong, W. Schwalb, Y. Wang, Y. Chen, Y. Tang, J. Si, B. Shirinzadeh and W. Cheng, *Nat. Commun.*, 2014, **5**, 3132.